Nanoscale Research Letters
a SpringerOpen Journal

NANO EXPRESS Open Access

Tunable insulator-quantum Hall transition in a weakly interacting two-dimensional electron system

Shun-Tsung Lo[1], Yi-Ting Wang[2], Sheng-Di Lin[3], Gottfried Strasser[4], Jonathan P Bird[5], Yang-Fang Chen[1,2] and Chi-Te Liang[1,2*]

Abstract

We have performed low-temperature measurements on a gated two-dimensional electron system in which electron–electron (e-e) interactions are insignificant. At low magnetic fields, disorder-driven movement of the crossing of longitudinal and Hall resistivities (ρ_{xx} and ρ_{xy}) can be observed. Interestingly, by applying different gate voltages, we demonstrate that such a crossing at $\rho_{xx} \sim \rho_{xy}$ can occur at a magnetic field higher, lower, or equal to the temperature-independent point in ρ_{xx} which corresponds to the direct insulator-quantum Hall transition. We explicitly show that $\rho_{xx} \sim \rho_{xy}$ occurs at the inverse of the classical Drude mobility $1/\mu_D$ rather than the crossing field corresponding to the insulator-quantum Hall transition. Moreover, we show that the background magnetoresistance can affect the transport properties of our device significantly. Thus, we suggest that great care must be taken when calculating the renormalized mobility caused by e-e interactions.

Keywords: Hall effect; Magnetoresistance; Electrons; Direct insulator-quantum hall transition

Background

At low temperatures (T), disorder and electron–electron (e-e) interactions may govern the transport properties of a two-dimensional electron system (2DES) in which electrons are confined in a layer of the nanoscale, leading to the appearance of new regimes of transport behavior [1]. In the presence of sufficiently strong disorder, a 2DES may behave as an insulator in the sense that its longitudinal resistivity (ρ_{xx}) decreases with increasing T [2]. It is useful to probe the intriguing features of this 2D insulating state by applying a magnetic field (B) perpendicular to the plane of a 2DES [2-4]. In particular, the direct transition from an insulator (I) to a high filling factor ($\nu \geq 3$) quantum Hall (QH) state continues to attract a great deal of both experimental [5-13] and theoretical [14-16] interest. This is motivated by the relevance of this transition to the zero-field metal-insulator transition [17] and by the insight it provides on the evolution of extended states at low magnetic fields. It has already been shown that the nature of the background disorder, in coexistence with e-e interactions, may influence the zero-field metallic behavior [18] and the QH plateau-plateau transitions [19,20]. However, studies focused on the direct I-QH transitions in a 2DES with different kinds of disorder are still lacking. Previously, we have studied a 2DES containing self-assembled InAs quantum dots [11], providing a predominantly short-range character to the disorder. We observed multiple T-independent points in $\rho_{xx}(B)$, indicating a series of transitions between a low-field insulator and a QH state. The oscillatory amplitude of $\rho_{xx}(B)$ was well fitted by the Shubnikov-de Haas (SdH) theory [21-23], with amplitude given by

$$\Delta\rho_{xx}(B,T) = C\exp\left(-\pi/\mu_q B\right)D(B,T), \quad (1)$$

where μ_q represents the quantum mobility, $D(B, T) = 2\pi^2 k_B m^* T/\hbar eB \sinh(2\pi^2 k_B m^* T/\hbar eB)$, and C is a constant relevant to the value of ρ_{xx} at $B = 0$ T. The observation of the SdH oscillations suggests the possible existence of a Fermi-liquid metal. It should be pointed

* Correspondence: ctliang@phys.ntu.edu.tw
[1]Graduate Institute of Applied Physics, National Taiwan University, Taipei 106, Taiwan
[2]Department of Physics, National Taiwan University, Taipei 106, Taiwan
Full list of author information is available at the end of the article

out that the SdH theory is derived by considering Landau quantization in the metallic regime without taking localization effects into account [24,25]. By observing the T-dependent Hall slope, however, the importance of e-e interactions in the metallic regime can be demonstrated [26]. In addition, as reported in [27], with a long-range scattering potential, SdH-type oscillations appear to span from the insulating to the QH-like regime when the e-e interaction correction is weak. Recently, the significance of percolation has been revealed both experimentally [28] and theoretically [29,30]. Therefore, to fully understand the direct I-QH transition, further studies on e-e interactions in the presence of background disorder are required.

At low B, quantum corrections resulting from weak localization (WL) and e-e interactions determine the temperature and magnetic field dependences of the conductivity, and both can lead to insulating behavior. The contribution of e-e interactions can be extracted after the suppression of WL at $B > B_{\mathrm{tr}}$, where the transport magnetic field (B_{tr}) is given by $\frac{\hbar}{4eD\tau}$ with reduced Planck's constant ($\hbar$), electron charge (e), diffusion constant (D), and transport relaxation time (τ). In systems with short-range potential fluctuations, the theory of e-e interactions is well established [31]. It is derived based on the interference of electron waves that follow different paths, one that is scattered off an impurity and another that is scattered by the potential oscillations (Friedel oscillation) created by all remaining electrons. The underlying physics is strongly related to the return probability of a scattered electron. In the diffusion regime ($k_{\mathrm{B}}T\tau/\hbar < < 1$ with Boltzmann constant k_{B}), e-e interactions contribute only to the longitudinal conductivity (σ_{xx}) without modifying the Hall conductivity (σ_{xy}). On the other hand, in the ballistic regime ($k_{\mathrm{B}}T\tau/\hbar > > 1$), e-e interactions contribute both to σ_{xx} and σ_{xy}, and effectively reduce to a renormalization of the transport mobility. However, the situation is different for long-range potential fluctuations, which are usually dominant in high-quality GaAs-based heterostructures in which the dopants are separated from the 2D electron gas by an undoped spacer. It is predicted that the interaction corrections can be suppressed at $B = 0$ but that they can eventually be restored at high magnetic fields $B > 1/\mu_{\mathrm{D}}$ with enhanced return probability of scattered electrons, where μ_{D} represents the Drude mobility [32,33]. Therefore, it is of great interest to study the direct insulator-quantum Hall transition in a system with long-range scattering, under which the e-e interactions can be sufficiently weak at low magnetic fields.

Theoretically, for either kind of background disorder, no specific feature of interaction correction is predicted in the intermediate regime where $k_{\mathrm{B}}T\tau/\hbar \approx 1$. Nevertheless, as generalized by Minkov et al. [34,35], electron–electron interactions can still be decomposed into two parts. One, with properties similar to that in the diffusion regime, is termed the diffusion component, whereas the other, sharing common features with that in the ballistic limit, is known as the ballistic component. Therefore, by considering the renormalized transport mobility μ' induced by the ballistic contribution and the diffusion correction $\delta\sigma_{xx}^{d}$, σ_{xx} is expressed as

$$\sigma_{xx} = \frac{ne\mu'}{1+\mu'^2B^2} + \delta\sigma_{xx}^{d}, \tag{2}$$

$$\sigma_{xy} = \frac{ne\mu'^2B}{1+\mu'^2B^2}. \tag{3}$$

It directly follows that the ballistic contribution $\delta\sigma_{xx}^{b}$ is given by $\delta\sigma_{xx}^{b} = ne(\mu' - \mu_D)$, where n is the electron density and μ_{D} is the transport mobility derived in the Drude model. After performing matrix inversion with the components given in Equations 2 and 3, the magnetoresistance $\rho_{\mathrm{xx}}(B)$ takes the parabolic form [36,37]

$$\rho_{xx} \approx \frac{1}{ne\mu'} - \frac{1}{(ne\mu')^2}\left(1-\mu'^2B^2\right)\delta\sigma_{xx}^{d} \tag{4}$$

The Hall slope R_{H} (ρ_{xy}/B with Hall resistivity ρ_{xy}) now becomes T-dependent which is ascribed to the diffusion correction $\delta\sigma_{xx}^{d}$ [38]. As will be shown later, Equations 3, 4, and 5 will be used to estimate the e-e interactions in our system. Moreover, both diffusive and ballistic parts will be studied.

As suggested by Huckestein [16], at the direct I-QH transition that is characterized by the approximately T-independent point in ρ_{xx},

$$\rho_{\mathrm{xx}} \sim \rho_{\mathrm{xy}} \tag{5}$$

While Equation 5 holds true in some experiments [2], in others it has been found that ρ_{xy} can be significantly higher than ρ_{xx} near the direct I-QH transition [10,28]. On the other hand, ρ_{xy} can also be lower than ρ_{xx} near the direct I-QH transition in some systems [39]. Therefore, it is interesting to explore if it is possible to tune the direct I-QH transition within the *same* system so as to study the validity of Equation 5. In the original work of Huckestein [16], e-e interactions were not considered. Therefore, it is highly desirable to study a weakly disordered system in which e-e interactions are insignificant. In this paper, we investigate the direct I-QH transition in the presence of a long-range scattering potential, which is exploited as a means to suppress e-e interactions. We are able to tune the direct I-QH transition so that the corresponding field for which Equation 5 is satisfied can be higher or lower than, or even equal, to the crossing field that corresponds to the direct I-QH transition. Interestingly, we show that the inverse Drude mobility $1/\mu_D$ is approximately equal to the field where ρ_{xx} crosses ρ_{xy}, rather than the one responsible for the direct I-QH transition. We also show that the onset of strong localization occurs at a relatively higher field which does not correspond to $1/\mu_D$.

Methods

A gated modulation-doped AlGaAs/GaAs heterostructure (LM4640) is used in our study. The following layer sequence was grown on a semi-insulating GaAs substrate: 1 μm GaAs, 200 nm $Al_{0.33}Ga_{0.67}As$, 40 nm Si-doped $Al_{0.33}Ga_{0.67}As$ with doping concentration in cubic centimeter, and finally a 10-nm GaAs cap layer. The sample was mesa etched into a standard Hall bar pattern, and a NiCr/Au gate was deposited on top of it by thermal evaporation. The length and width of the Hall bars are 640 and 80 μm, respectively. Four-terminal magnetotransport measurements were performed in a top-loading He^3 system using standard ac phase-sensitive lock-in techniques over the temperature range 0.32 K ≤ T ≤16 K at three different gate voltages V_g = −0.125, −0.145, and −0.165 V.

Results and discussion

Figure 1a shows $\rho_{xx}(B)$ and $\rho_{xy}(B)$ at various T for V_g = −0.145 V. It can be seen from the inset in Figure 1 that the 2DES behaves as an insulator over the whole temperature range at all applied gate voltages. The Hall slope R_H shows a weak T dependence below T = 4 K and is approximately constant at high T, which can be seen clearly in Figure 1b for each V_g. For 1.84 T < B < 2.85 T, a well-developed ν = 2 QH state manifests itself in the quantized ν = 2 Hall plateau and the associated vanishing of ρ_{xx}. In order to study the transition from an insulator to a QH state, detailed results of ρ_{xx} and ρ_{xy} at low T are shown in Figure 2a,b,c for each V_g, and the converted σ_{xx} and σ_{xy} are presented in Figure 3. At V_g = −0.125 V, spin splitting is resolved as the effective disorder is decreased compared to that at V_g = −0.145 and −0.165 V. The reason for this is that the carrier density at V_g = −0.125 V is higher than those at V_g = −0.145 and −0.165 V. Following the suppression of weak localization, with its sharp negative magnetoresistance (NMR) at low magnetic fields, the 2DES undergoes a direct I-QH at B = 0.26, 0.26, and 0.29 T ≡ B_c for V_g = −0.125, −0.145, and −0.165 V, respectively, since there is no signature of ν = 2 or ν = 1 QH state near B_c. We note that in all cases, B_c > 10 B_{tr}. Therefore, it is believed that near the crossing field, weak localization effect is not significant in our system [37]. It is of fundamental

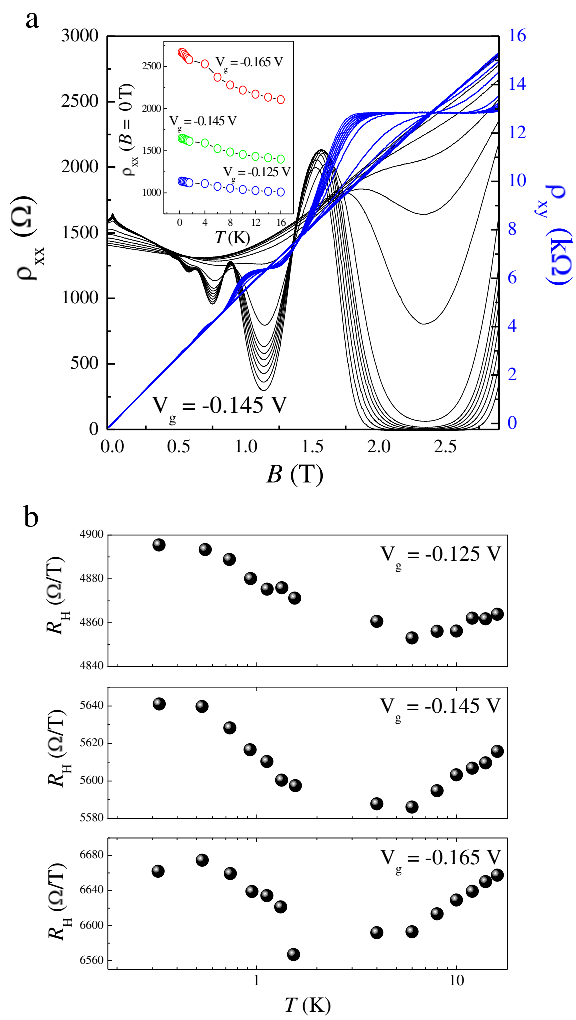

Figure 1 Temperature dependence. (a) Longitudinal and Hall resistivities (ρ_{xx} and ρ_{xy}) as functions of magnetic field B at various temperatures T ranging from 0.3 to 16 K. The inset shows $\rho_{xx}(B = 0, T)$ at three applied gate voltages. **(b)** Hall slope R_H as a function of T at each V_g on a semi-logarithmic scale.

interest to see in Figure 2d that the relative position of B_c with respect to that corresponding to the crossing of ρ_{xx} and ρ_{xy} is not necessarily equal. Following the transition, magneto-oscillations superimposed on the background of NMR are observed within the range 0.46 T ≤ B ≤ 1.03 T, 0.49 T ≤ B ≤ 1.12 T, and 0.53 T ≤ B ≤ 0.94 T for corresponding V_g, the oscillating amplitudes of which are all well fitted by Equation 1. The results are shown in Figure 4a,b,c for three different V_g. The good agreement with the SdH theory suggests that strong localization effects are not significant near B_c. This is consistent with our previous results, performed on both a delta-doped quantum well with additional modulation doping [13] and a modulation-doped AlGaAs/GaAs heterostructure with a superlattice structure [27]. It

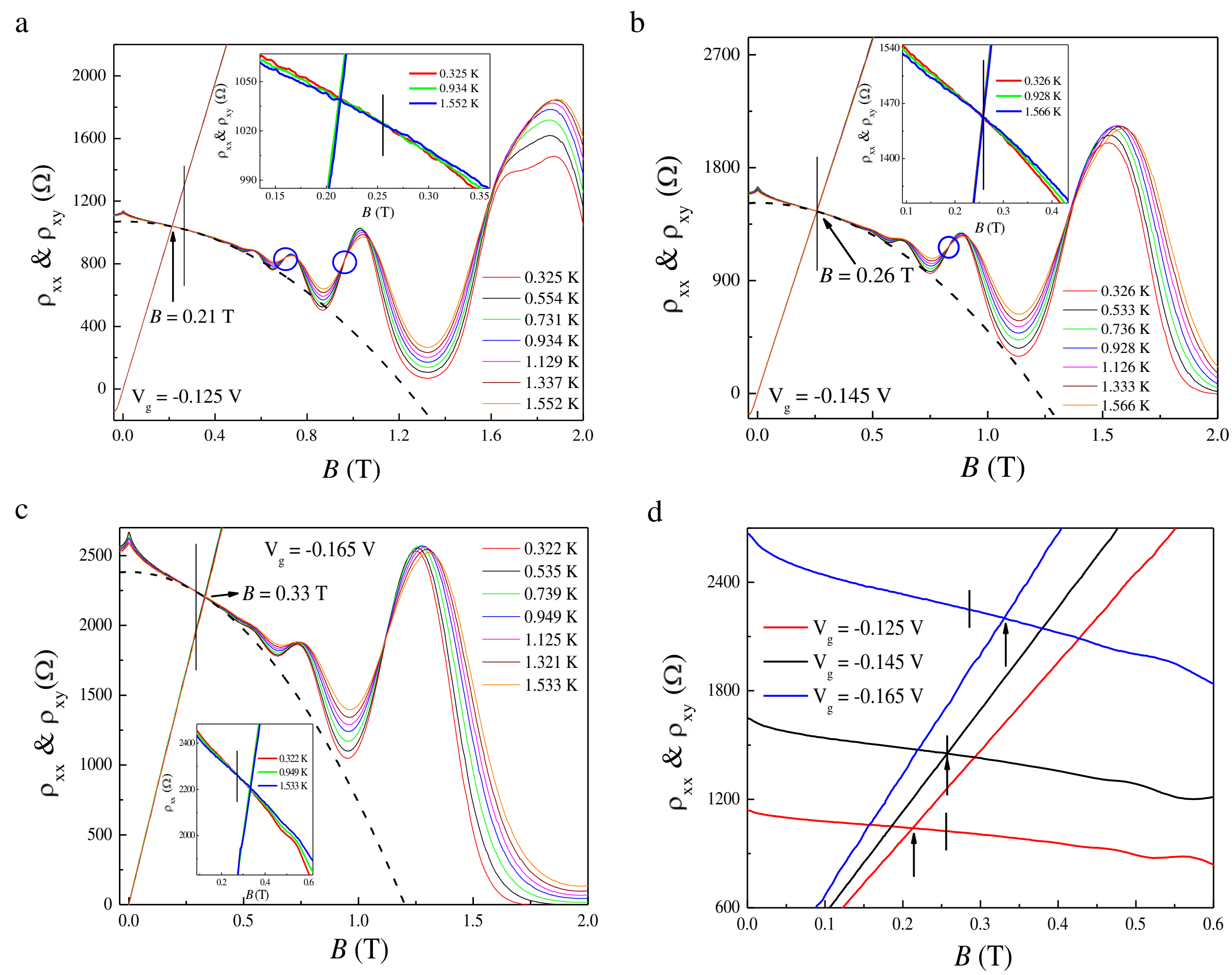

Figure 2 Detailed results of ρ_{xx} and ρ_{xy} at low *T*. The *B* dependences of ρ_{xx} and ρ_{xy} at various *T* ranging from 0.3 to 1.5 K for **(a)** V_g = −0.125 V, **(b)** V_g =−0.145 V, and **(c)** V_g = −0.165 V. The insets are the zoom-ins of low-field $\rho_{xx}(B)$. The dashed lines are the fits to Equation 4 at the lowest *T*. For comparison, the results at the lowest *T* for each V_g are re-plotted in **(d)**. The *T*-independent points corresponding to the direct I-QH transition are indicated by vertical lines, and those for the crossings of ρ_{xx} and ρ_{xy} are denoted by arrows. Other *T*-independent points are indicated by circles.

follows that we can obtain the quantum mobility μ_q from the fits, which is expected to be an essential quantity regarding Landau quantization. The estimated μ_q are 0.88, 0.84, and 0.77 m^2/Vs for V_g = −0.125, −0.145, and −0.165 V, respectively. Moreover, from the oscillating period in 1/*B*, the carrier density *n* is shown to be *T*-independent such that a slight decrease in R_H at low *T* does not result from the enhancement of carrier density *n*. Instead, these results can be ascribed to e-e interactions.

At first glance, the *T*-dependent R_H, together with the parabolic MR in ρ_{xx} (denoted by the dashed lines in Figure 2 for each V_g), indicates that e-e interactions play an important role in our system. However, as will be shown later, the corrections provided by the diffusion and ballistic part of e-e interactions have opposite sign to each other, such that a cancelation of e-e interactions can be realized. Here we use two methods to analyze the contribution of e-e interactions. The first method is by fitting the measured ρ_{xx} to Equation 4, as shown by the blue symbols in Figure 5, from which we can obtain both $\delta\sigma_{xx}^b$ and $\delta\sigma_{xx}^d$. The value of $\delta\sigma_{xx}^d$ is shown to be negative, as a result of the observed negative MR. We can see clearly from the dashed line in Figure 2 that the parabolic MR fits Equation 4 well at $B > B_c$ but that it cannot be extended to the field where SdH oscillations occur. The obtained μ', with an approximately linear dependence on *T* that is characteristic of the ballistic contribution of e-e interactions, is shown in Figure 6a,b,c for V_g = −0.125, −0.145, and −0.165 V, respectively. It should be mentioned that we cannot use this method to

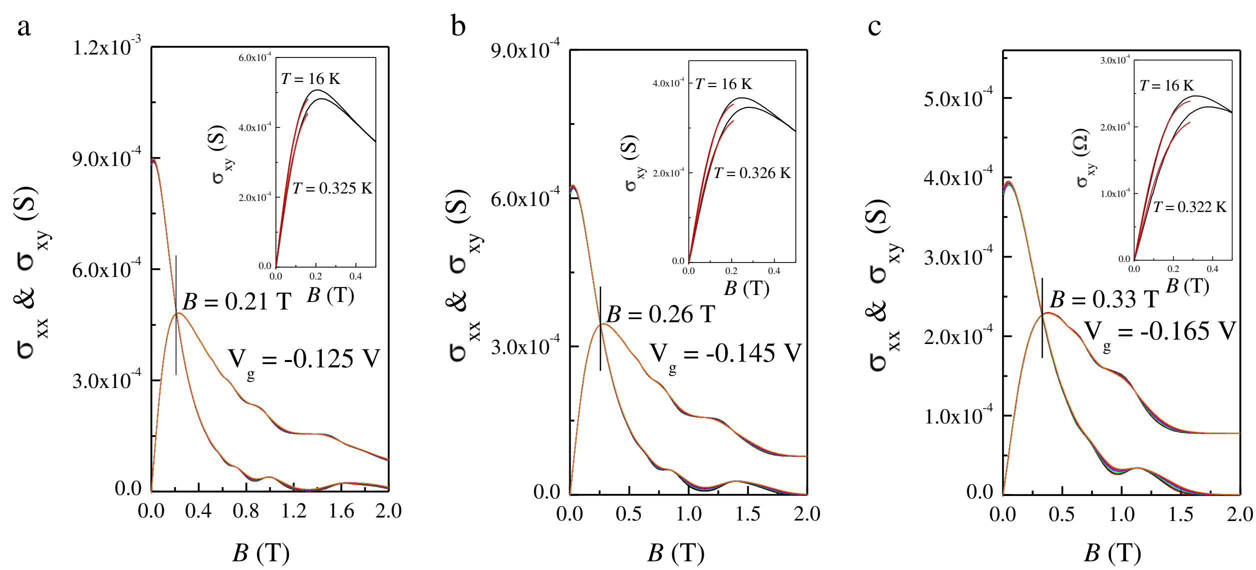

Figure 3 Converted $\sigma_{xx}(B)$ and $\sigma_{xy}(B)$ at various T ranging from 0.3 to 1.5 K. For **(a)** $V_g = -0.125$ V, **(b)** $V_g = -0.145$ V, and **(c)** $V_g = -0.165$ V. The insets show $\sigma_{xy}(B)$ at $T = 0.3$ K and $T = 16$ K together with the fits to Equation 3 as indicated by the red lines. The vertical lines point out the crossings of σ_{xx} and σ_{xy}.

obtain μ' for $T > 4$ K since there is no apparent parabolic NMR, as shown in Figure 1a. The second method is based on the analysis of σ_{xy} using Equation 3, as shown in the inset to Figure 3 at the highest and lowest measured T. In this approach, n is determined from the SdH oscillations, from which the renormalized mobility can also be obtained at high T even without the parabolic negative MR induced by the diffusion correction. Here we limit the fitting intervals below 0.75 B_{max} to avoid the regime near $\mu_D B \sim 1$, where B_{max} denotes the

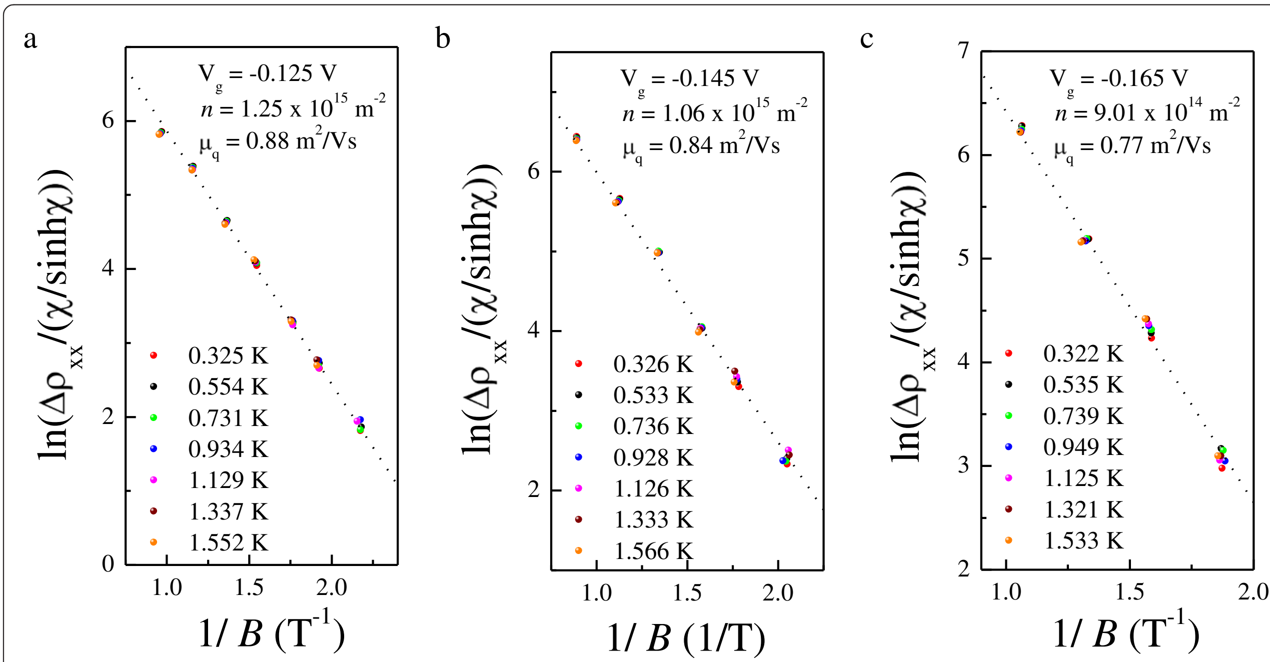

Figure 4 ln ($\Delta\rho_{xx}(B, T)/D(B, T)$) as a function of 1/$B$. For **(a)** $V_g = -0.125$ V, **(b)** $V_g = -0.145$ V, and **(c)** $V_g = -0.165$ V. The dotted lines are the fits to Equation 1.

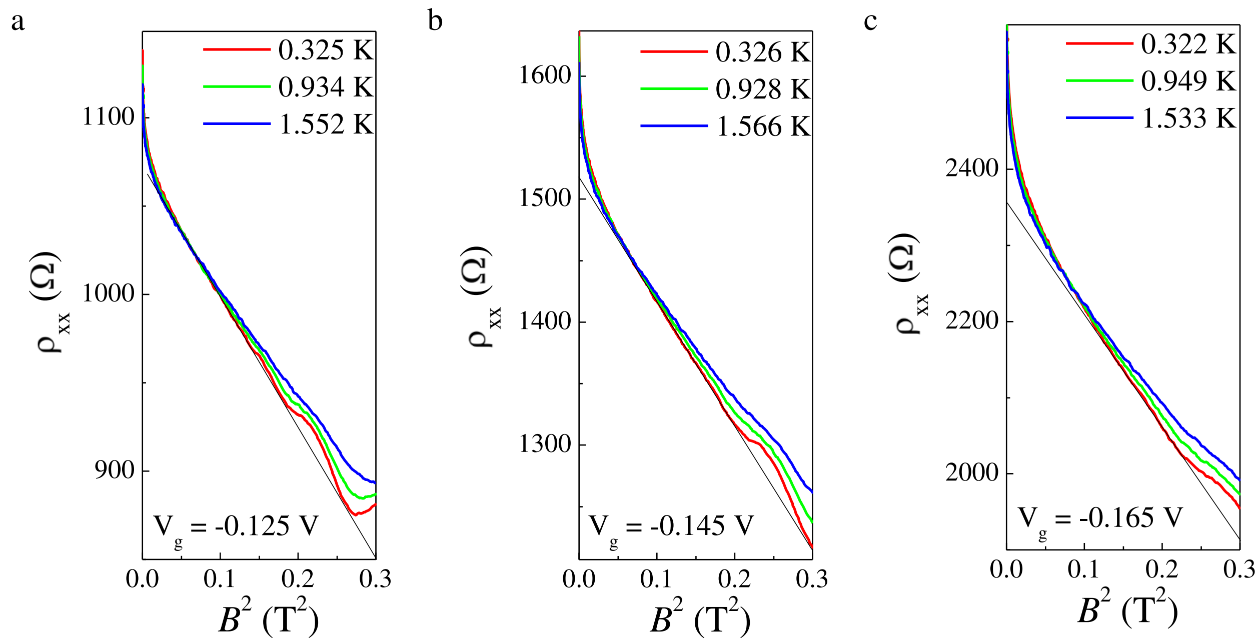

Figure 5 ρ_{xx} **as a function of** B^2 **for** V_g **= −0.125 (a), −0.145 (b), and−0.165 (c) V.** The straight lines are provided as a guide to the eye to show the quadratic dependence on *B*.

field corresponding to the appearance of maximum σ_{xy} at the lowest T. The fitting results are plotted at each V_g as red symbols in Figure 6, allowing a comparison with those obtained by the first method. The figures show that μ' is proportional to T when $T > 4$ K. There is a clear discrepancy between the values obtained from the different fits at a relatively lower magnitude of V_g, which can be ascribed to the background MR (as will be discussed further below). Nevertheless, both cases indicate that the ballistic contribution, defined as $\delta\sigma_{xx}^{b} = ne$

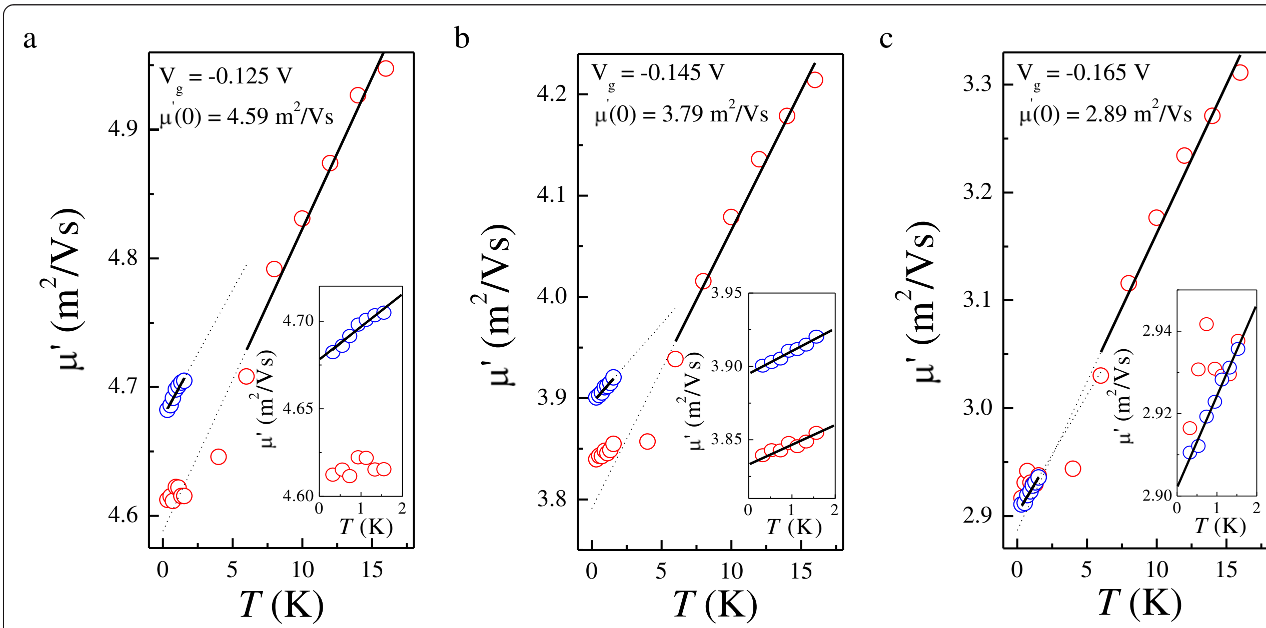

Figure 6 Renormalized mobility μ' **as a function of** T **for** V_g **= −0.125 (a), −0.145 (b), and−0.165 (c) V.** The red and blue symbols denote the results obtained from the fits according to Equations 3 and 4, respectively. The insets are the zoom-ins of low-*T* results. The dotted lines represent the linear extrapolation of straight lines at $T > 4$ K.

$(\mu'-\mu_D)$ with $\mu_D \equiv \mu(T = 0K)$, has positive sign and therefore results in a partial cancelation of the diffusion correction. This is consistent with the prediction that the influence of e-e interactions is weakened in systems with long-range scattering potentials.

At high magnetic fields $B > 1/\mu_D$, semiclassical effects should affect the background resistance, resulting in either positive or negative MR [40,41]. Therefore, it is not possible to obtain reliable values for μ' from the first method. Here we use the value of $\mu'(T = 0\text{K})$, obtained by linearly extrapolating the high-T results from the second method to $T = 0$ K [27,34], to estimate μ_D and so as to allow a discussion on the role of the non-oscillatory background. As demonstrated in Figure 6, the estimated values of μ_D are 4.59, 3.79, and 2.89 m^2/Vs for V_g = −0.125, −0.145, and −0.165 V, respectively, from which the corresponding ratios of μ_D/μ_q (5.22, 4.51, and 3.75) are determined with μ_q obtained by analyzing the amplitudes of SdH oscillations as shown in Figure 3. Since μ_q counts all scattering events whereas μ_D is sensitive only to large-angle ones, we can deduce the predominant scattering mechanism in a 2DES from the value of μ_D/μ_q [42-44]. We can see from Figure 6 that both methods give the same results at low T for V_g = −0.165 V, implying that the influence of background MR is diminished as the amount of short-range scattering potential is increased. In what follows, we will focus on the issue about direct I-QH transitions.

Huckestein has suggested that the direct I-QH transition can be identified as a crossover from weak localization to the onset of Landau quantization, resulting in a strong reduction of the conductivity. The field $B \sim 1/\mu$ separates these two regions which are characterized by opposite T dependences and are characterized by $\rho_{xx} \sim \rho_{xy}$. In his argument, μ is taken to be the transport mobility. Nevertheless, recent experimental results [11-13] demonstrate that different mobilities should be introduced to understand transport near a direct I-QH transition; the observed direct I-QH transition can be irrelevant to Landau quantization, while Landau quantization does not always cause the formation of QH states. Furthermore, it has already been demonstrated in various kinds of 2DES that the crossing point $\rho_{xx} = \rho_{xy}$ can occur before or after the appearance of the T-independent point that corresponds to a direct I-QH transition. Moreover, the strongly T-dependent Hall slope induced by e-e interactions may affect the position of $\rho_{xx} = \rho_{xy}$ at different T. As shown in Figure 2b for V_g = −0.145 V, the direct I-QH transition characterized by an approximately T-independent crossing point B_c in ρ_{xx} does occur at the field where $\rho_{xx} \sim \rho_{xy}$ even though ρ_{xy} slightly depends on T. In addition, the inverse of the estimated Drude mobility $1/\mu_D \sim 0.26$ T is found to be close to B_c. To this extent, Huckestein's model seems to be reasonable. However, we can see that there are no apparent oscillations in ρ_{xx} around B_c and that the onset of strong localization occurs at $B > 1.37$ T, as characterized by a well-quantized $\nu = 2$ Hall plateau and vanishing ρ_{xx} with increasing B, more than five times larger than B_c. In order to test the validity of the relation $\rho_{xx} \sim \rho_{xy}$ at B_c, different gate voltages were applied to vary the

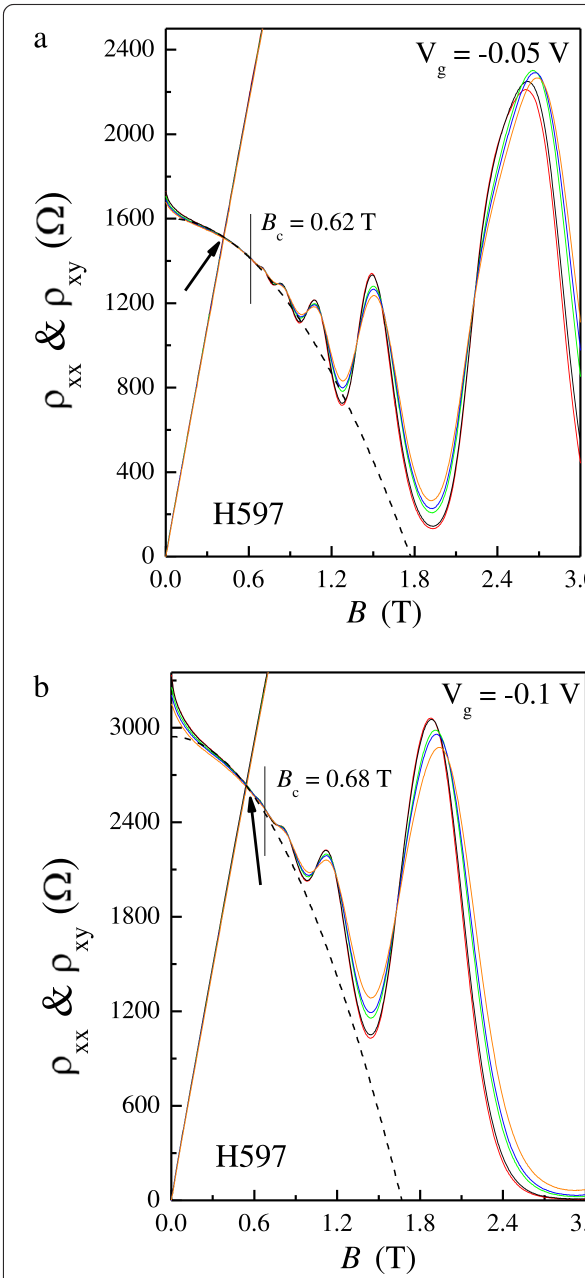

Figure 7 ρ_{xx} and ρ_{xy} as functions of B at various T ranging from 0.3 to 2 K. For **(a)** V_g = −0.05 V and **(b)** V_g = −0.1 V.

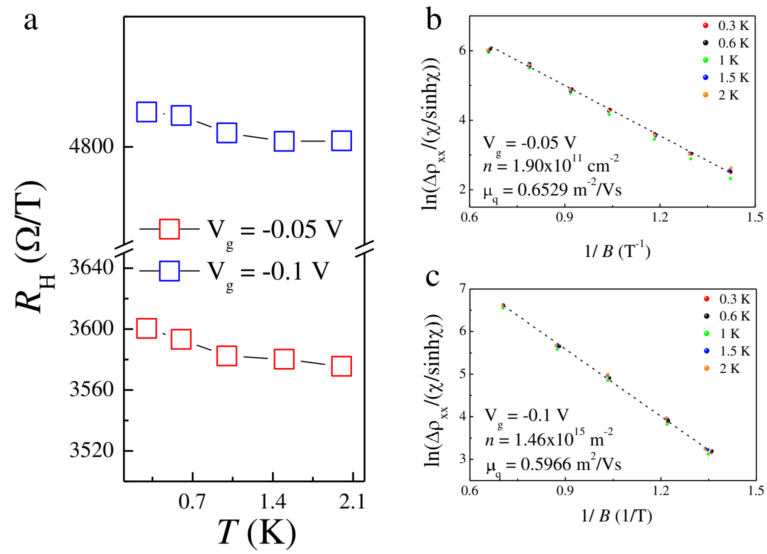

Figure 8 R_H **and ln(**$\Delta\rho_{xx}(B, T)/D(B, T)$**). (a)** R_H as a function of T for both gate voltages. ln($\Delta\rho_{xx}(B, T)/D(B, T)$) as a function of 1/$B$ is shown in **(b)** and **(c)** for V_g = −0.05 and −0.1 V, respectively. The dotted lines are the fits to Equation 1.

effective amount of disorder and carrier density in the 2DES. As shown in Figure 2a, by increasing V_g to −0.125 V, ρ_{xx} becomes smaller than ρ_{xy} at $B_c \sim 0.26$ T, while $\rho_{xx} \sim \rho_{xy}$ at a smaller field of approximately 0.21 T, which is shown to be close to $1/\mu_D \sim 0.22$ T rather than B_c. Moreover, by decreasing V_g to −0.165 V, $\rho_{xx} \sim \rho_{xy}$ appears at $B \sim 0.33$ T which is larger than $B_c \sim 0.29$ T, as shown in Figure 2c. The inverse Drude mobility $1/\mu_D \sim 0.35$ is also found to be close to the field where $\rho_{xx} \sim \rho_{xy}$ under this gate voltage. In all three cases, the crossings of σ_{xx} and σ_{xy} coincide with those of ρ_{xx} and ρ_{xy}, as shown in Figure 2 for each V_g. Therefore, our studies suggest that the field where $\rho_{xx} \sim \rho_{xy}$ is governed by $1/\mu_D$ and does not always correspond to that responsible for a direct I-QH transition as the influence of e-e interactions is not significant. As a result, $\rho_{xx} \sim \rho_{xy}$ can occur on both sides of B_c as seen clearly in Figure 2d.

Interestingly, in the crossover from SdH oscillations to the QH state, we observe additional T-independent points, labeled by circles in Figure 2 for each V_g, other than the one corresponding to the onset of strong localization. As shown in Figure 2a for V_g = −0.125 V, the resistivity peaks at around B = 0.73 and 1.03 T appear to move with increasing T, a feature of the scaling behavior [7] of standard QH theory around the crossing points B = 0.70 and 0.96 T, respectively. Therefore, survival of the SdH theory for 0.46 T ≤ B ≤ 1.03 T reveals that semiclassical metallic transport may coexist with quantum localization. The superimposed background MR may be the reason

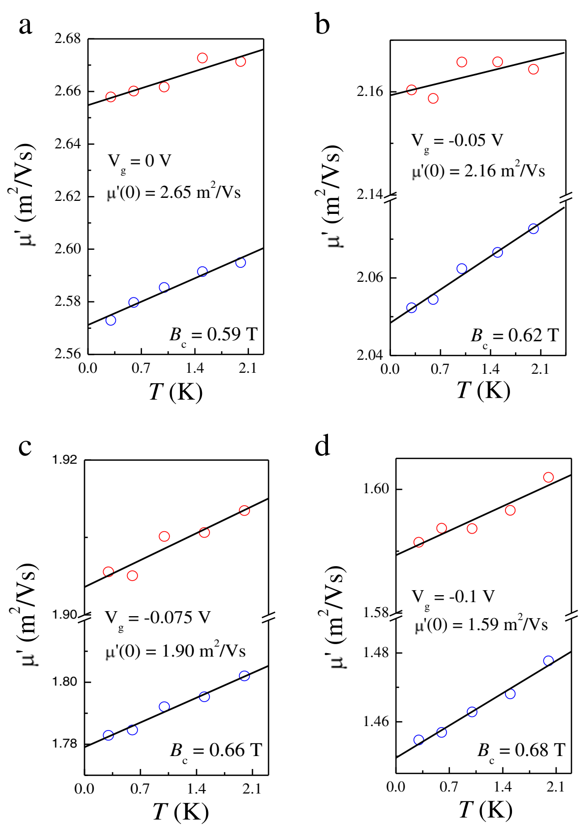

Figure 9 μ' **as a function of** T**.** For **(a)** V_g = 0 V, **(b)** V_g = −0.05 V, **(c)** V_g = −0.075 V, and **(d)** V_g = −0.1 V. The symbols are the same as those used in Figure 6.

for this coexistence, which is demonstrated by the upturned deviation from the parabolic dependence as shown in Figure 2a [45]. Therefore, it is reasonable to attribute the overestimated μ' shown by the blue symbols in Figure 5a to the influence of the background MR. Similar behavior can also be found for V_g = −0.145 V even though spin splitting is unresolved, indicating that the contribution of background MR mostly comes from semiclassical effects. However, such a crossing point cannot be observed for V_g = −0.165 V since there is no clear separation between extended and localized states with strong disorder. Only a single T-independent point corresponding to the onset of strong localization occurs at B = 1.12 T.

In order to check the validity of our present results, further experiments were performed on a device (H597) with nominally T-independent Hall slope at different applied gate voltages [27]. As shown in Figure 7a for V_g = −0.05 V, weakly insulating behavior occurs as $B < 0.62$ T ≡ B_c, which corresponds to the direct I-QH transition since there is no evidence of the $\nu = 1$ or $\nu = 2$ QH state near B_c. The crossing of ρ_{xx} and ρ_{xy} is found to occur at $B \sim 0.5$ T which is smaller than B_c. As we decrease V_g to −0.1 V, thereby increasing the effective amount of disorder in the 2DES, the relative positions between these two fields remain the same as shown in Figure 7b. Nevertheless, it can be observed that ρ_{xy} tends to move closer to ρ_{xx} with decreasing V_g. This may be quantified by defining the ratio ρ_{xy}/ρ_{xx} at B_c, whose value is 1.57 and 1.31 for V_g = −0.05 and −0.1 V, respectively.

The interaction-induced parabolic NMR can be observed at both gate voltages. This result, together with the negligible T dependence of the Hall slope as shown in Figure 8a, implies that the ballistic part of the e-e interactions dominates as mentioned above. Therefore, by analyzing the observed parabolic NMR and corresponding Hall conductivity with Equations 4 and 3, respectively, we can obtain the renormalized transport mobilities μ' at each measured T. Again, the estimated μ' obtained by different methods as shown using different symbols in Figure 9 do not coincide with each other. It has already been demonstrated that the background MR can validate the SdH theory at $B > 1/\mu_q$ for V_g = −0.075 V in [27]. However, as shown in Figure 9c for V_g = −0.1 V, $1/\mu_q \sim 1.67$ T is found to be close to the crossing point in ρ_{xx} at $B \sim 1.63$ T, which corresponds to the $\nu = 4$ to $\nu = 2$ QH plateau-plateau transition. Therefore, it is reasonable to attribute the discrepancy of μ' obtained by different methods to the background MR. However, we can see that the value of μ' is underestimated by using the first method, which is different from that in sample LM4640 with the overestimated result. Our experimental results in conjunction with existing reports [37,45-48] suggest that a detailed treatment of the background MR is required. Moreover, the role of spin splitting does not seem to be significant in our system [49-51].

The inverse Drude mobilities $1/\mu_D$ estimated by the same procedures are 0.38, 0.46, 0.53, and 0.63 T for V_g = 0, −0.05, −0.075, and −0.1 V, respectively. We can see clearly that $1/\mu_D$ deviates from the crossing of ρ_{xx} and ρ_{xy} (0.35, 0.43, 0.47, and 0.54 T for the corresponding V_g) as the applied gate voltage is decreased. The enhancement of background disorder with decreasing V_g may be the reason for such a discrepancy which can be deduced from the ratio μ_D/μ_q (4.27, 3.32, 2.92, and 2.65 for the corresponding V_g). The underlying physics is that the interference-induced e-e interactions are regained as a sufficient amount of short-range scattering potential is introduced, which leads to increased electron backscattering. Moreover, the parabolic NMR extending well below $1/\mu_D$, as shown in Figure 7, provides another evidence for the recovery of e-e interactions since in a 2DES dominated by a long-range scattering potential, it occurs only as $B > 1/\mu_D$. We hope that our results will stimulate further investigations to fully understand the evolution of extended states near $\mu_D B = 1$ in a disordered 2DES both experimentally and theoretically.

Conclusion

In conclusion, we have studied magnetotransport in gated two-dimensional electron systems. By varying the effective amount of disorder and the carrier density through different applied gate voltages, we observe that the crossing of ρ_{xx} and ρ_{xy} is governed by the inverse of the Drude mobility $1/\mu_D$ and can occur for $B > B_c$, $B < B_c$, and $B \sim B_c$ where B_c corresponds to the direct I-QH transition as the influence of e-e interactions is not significant. However, such a criterion breaks down when a sufficient amount of disorder is introduced, which leads to the recovery of interference-induced e-e interactions. Moreover, our results demonstrate that the magneto-oscillations following the semiclassical SdH theory can coexist with quantum localization as a result of the background MR, and the onset of strong localization occurs at a much higher field than either B_c or $1/\mu_D$. Therefore, in order to obtain a thorough understanding of the ground state of a weakly interacting 2DES, it is essential to eliminate the influence of e-e interactions as much as possible.

Competing interests

The authors declare that they have no competing interests.

Authors' contributions

STL and YTW performed the experiments. GS and SDL prepared the devices. YFC and CTL coordinated the project. STL, JPB, and CTL drafted the paper. All the authors read and approved the final version of the manuscript.

Acknowledgment

This work was funded by National Taiwan University (grant no. 102R7552-2).

Author details

[1]Graduate Institute of Applied Physics, National Taiwan University, Taipei 106, Taiwan. [2]Department of Physics, National Taiwan University, Taipei 106, Taiwan. [3]Department of Electronics Engineering, National Chiao Tung University, Hsinchu 300, Taiwan. [4]Institute for Solid State Electronics and Center for Micro- and Nanostructures, Technische Universität Wien, Floragasse 7, 1040, Vienna, Austria. [5]Department of Electrical Engineering, University at Buffalo, The State University of New York, Buffalo, New York 14260-1920, USA.

Received: 7 May 2013 Accepted: 26 June 2013
Published: 3 July 2013

References

1. Lee PA, Ramakrishnan TV: Disordered electronic systems. *Rev Mod Phys* 1985, 57:287.
2. Song SH, Shahar D, Tsui DC, Xie YH, Monroe D: New universality at the magnetic field driven insulator to integer quantum Hall effect transitions. *Phys Rev Lett* 1997, 78:2200.
3. Jiang HW, Johnson CE, Wang KL, Hannahs ST: Observation of magnetic-field-induced delocalization: transition from Anderson insulator to quantum Hall conductor. *Phys Rev Lett* 1993, 71:1439.
4. Hughes RJF, Nicholls JT, Frost JEF, Linfield EH, Pepper M, Ford CJB, Ritchie DA, Jones GAC, Kogan E, Kaveh M: Magnetic-field-induced insulator-quantum Hall-insulator transition in a disordered two-dimensional electron gas. *J Phys Condens Matter* 1994, 6:4763.
5. Lee CH, Chang YH, Suen YW, Lin HH: Magnetic-field-induced insulator-quantum Hall conductor-insulator transitions in doped GaAs/$Al_xGa_{1-x}As$ quantum wells. *Phys Rev B* 1997, 56:15238.
6. Smorchkova IP, Samarth N, Kikkawa JM, Awschalom DD: Giant magnetoresistance and quantum phase transitions in strongly localized magnetic two-dimensional electron gases. *Phys Rev B* 1998, 58:R4238.
7. Huang CF, Chang YH, Lee CH, Chou HT, Yeh HD, Liang C-T, Chen YF, Lin HH, Cheng HH, Hwang GJ: Insulator-quantum Hall conductor transitions at low magnetic field. *Phys Rev B* 2002, 65:045303.
8. Kim G-H, Liang C-T, Huang CF, Lee MH, Nicholls JT, Ritchie DA: Insulator-quantum Hall transitions in two-dimensional electron gas containing self-assembled InAs dots. *Physica E* 2003, 17:292.
9. Kim G-H, Liang C-T, Huang CF, Nicholls JT, Ritchie DA, Kim PS, Oh CH, Juang JR, Chang YH: From localization to Landau quantization in a two-dimensional GaAs electron system containing self-assembled InAs quantum dots. *Phys Rev B* 2004, 69:073311.
10. Huang T-Y, Juang JR, Huang CF, Kim G-H, Huang C-P, Liang C-T, Chang YH, Chen YF, Lee Y, Ritchie DA: On the low-field insulator-quantum Hall conductor transitions. *Physica E* 2004, 22:240.
11. Huang TY, Liang C-T, Kim G-H, Huang CF, Huang CP, Lin JY, Goan HS, Ritchie DA: From insulator to quantum Hall liquid at low magnetic fields. *Phys Rev B* 2008, 78:113305.
12. Chen KY, Chang YH, Liang C-T, Aoki N, Ochiai Y, Huang CF, Lin L-H, Cheng KA, Cheng HH, Lin HH, Wu JY, Lin S-D: Probing Landau quantization with the presence of insulator–quantum Hall transition in a GaAs two-dimensional electron system. *J Phys Condens Matter* 2008, 20:295223.
13. Lo ST, Chen KY, Lin TL, Lin LH, Luo DS, Ochiai Y, Aoki N, Wang Y-T, Peng ZF, Lin Y, Chen JC, Lin SD, Huang CF, Liang CT: Probing the onset of strong localization and electron–electron interactions with the presence of a direct insulator–quantum Hall transition. *Solid State Commun* 1902, 2010:150.
14. Liu DZ, Xie XC, Niu Q: Weak field phase diagram for an integer quantum Hall liquid. *Phys Rev Lett* 1996, 76:975.
15. Sheng DN, Weng ZY: Phase diagram of the integer quantum Hall effect. *Phys Rev B* 2000, 62:15363.
16. Huckestein B: Quantum Hall effect at low magnetic fields. *Phys Rev Lett* 2000, 84:3141.
17. Hanein Y, Nenadovic N, Shahar D, Shtrikman H, Yoon I, Li CC, Tsui DC: Linking insulator-to-metal transitions at zero and finite magnetic fields. *Nature* 1999, 400:735.
18. Clarke WR, Yasin CE, Hamilton AR, Micolich AP, Simmons MY, Muraki K, Hirayama Y, Pepper M, Ritchie DA: Impact of long- and short-range disorder on the metallic behaviour of two-dimensional systems. *Nat Phys* 2008, 4:55.
19. Ilani S, Martin J, Teitelbaum E, Smet JH, Mahalu D, Umansky V, Yacoby A: The microscopic nature of localization in the quantum Hall effect. *Nature* 2004, 427:328.
20. Amado M, Diez E, Lopez-Romero D, Rossella F, Caridad JM, Dionigi F, Bellani V, Maude DK: Plateau–insulator transition in graphene. *New J Phys* 2010, 12:053004.
21. Fowler AB, Fang FF, Howard WE, Stiles PJ: Magneto-oscillatory conductance in silicon surfaces. *Phys Rev Lett* 1966, 16:901.
22. Ando T: Theory of quantum transport in a two-dimensional electron system under magnetic fields. IV. Oscillatory conductivity. *J Phys Soc Jpn* 1974, 37:1233.
23. Coleridge PT, Zawadzki P, Sachrajda AS: Peak values of resistivity in high-mobility quantum-Hall-effect samples. *Phys Rev B* 1994, 49:10798.
24. Martin GW, Maslov DL, Reizer MY: Quantum magneto-oscillations in a two-dimensional Fermi liquid. *Phys Rev B* 2003, 68:241309.
25. Hang DR, Huang CF, Cheng KA: Probing semiclassical magneto-oscillations in the low-field quantum Hall effect. *Phys Rev B* 2009, 80:085312.
26. Huang TY, Liang C-T, Kim G-H, Huang CF, Huang CP, Ritchie DA: Probing two-dimensional metallic-like and localization effects at low magnetic fields. *Physica E* 2010, 42:1142.
27. Lo S-T, Wang Y-T, Bohra G, Comfort GE, Lin T-Y, Kang M-G, Strasser G, Bird JP, Huang CF, Lin L-H, Chen JC, Liang C-T: Insulator, semiclassical oscillations and quantum Hall liquids at low magnetic fields. *J Phys Condens Matter* 2012, 24:405601.
28. Gao KH, Yu G, Zhou YM, Wei LM, Lin T, Shang LY, Sun L, Yang R, Zhou WZ, Dai N, Chu JH, Austing DG, Gu Y, Zhang YG: Insulator-quantum Hall conductor transition in high electron density gated InGaAs/InAlAs quantum wells. *J Appl Phys* 2010, 108:063701.
29. Dubi Y, Meir Y, Avishai Y: Quantum Hall criticality, superconductor-insulator transition, and quantum percolation. *Phys Rev B* 2005, 71:125311.
30. Dubi Y, Meir Y, Avishai Y: Unifying model for several classes of two-dimensional phase transition. *Phys Rev Lett* 2005, 94:156406.
31. Zala G, Narozhny BN, Aleiner IL: Interaction corrections at intermediate temperatures: longitudinal conductivity and kinetic equation. *Phys Rev B* 2001, 64:214204.
32. Gornyi IV, Mirlin AD: Interaction-induced magnetoresistance: from the diffusive to the ballistic regime. *Phys Rev Lett* 2003, 90:076801.
33. Gornyi IV, Mirlin AD: Interaction-induced magnetoresistance in a two-dimensional electron gas. *Phys Rev B* 2004, 69:045313.
34. Minkov GM, Germanenko AV, Rut OE, Sherstobitov AA, Larionova VA, Bakarov AK, Zvonkov BN: Diffusion and ballistic contributions of the interaction correction to the conductivity of a two-dimensional electron gas. *Phys Rev B* 2006, 74:045314.
35. Minkov GM, Germanenko AV, Rut OE, Sherstobitov AA, Zvonkov BN: Renormalization of hole-hole interaction at decreasing Drude conductivity: gated GaAs/$In_xGa_{1-x}As$/GaAs heterostructures. *Phys Rev B* 2007, 76:165314.
36. Paalanen MA, Tsui DC, Hwang JCM: Parabolic magnetoresistance from the interaction effect in a two-dimensional electron gas. *Phys Rev Lett* 1983, 51:2226.
37. Li L, Proskuryakov YY, Savchenko AK, Linfield EH, Ritchie DA: Magnetoresistance of a 2D electron gas caused by electron interactions in the transition from the diffusive to the ballistic regime. *Phys Rev Lett* 2003, 90:076802.
38. Simmons MY, Hamilton AR, Pepper M, Linfield EH, Rose PD, Ritchie DA: Weak localization, hole-hole interactions, and the "metal"-insulator transition in two dimensions. *Phys Rev Lett* 2000, 84:2489.
39. Hilke M, Shahar D, Song SH, Tsui DC, Xie YH: Phase diagram of the integer quantum Hall effect in p-type germanium. *Phys Rev B* 2000, 62:6940.
40. Mirlin AD, Polyakov DG, Evers F, Wölfle P: Quasiclassical negative magnetoresistance of a 2D electron gas: interplay of strong scatterers and smooth disorder. *Phys Rev Lett* 2001, 87:126805.
41. Renard V, Kvon ZD, Gusev GM, Portal JC: Large positive magnetoresistance in a high-mobility two-dimensional electron gas: interplay of short- and long-range disorder. *Phys Rev B* 2004, 70:033303.
42. Harrang JP, Higgins RJ, Goodall RK, Jay PR, Laviron M, Delescluse P: Quantum and classical mobility determination of the dominant scattering mechanism in the two-dimensional electron gas of an AlGaAs/GaAs heterojunction. *Phys Rev B* 1985, 32:8126.
43. Das Sarma S, Stern F: Single-particle relaxation time versus scattering time in an impure electron gas. *Phys Rev B* 1985, 32:8442.

44. Coleridge PT, Stoner R, Fletcher R: **Low-field transport coefficients in $GaAs/Ga_{1-x}Al_xAs$ heterostructures.** *Phys Rev B* 1989, **39:**1120.
45. Gao KH, Zhou WZ, Zhou YM, Yu G, Lin T, Guo SL, Chu JH, Dai N, Gu Y, Zhang YG, Austing DG: **Magnetoresistance in high-density two-dimensional electron gas confined in InAlAs/InGaAs quantum well.** *Appl Phys Lett* 2009, **94:**152107.
46. Hang DR, Liang C-T, Juang JR, Huang T-Y, Hung WK, Chen YF, Kim G-H, Lee J-H, Lee J-H: **Electrically detected and microwave-modulated Shubnikov-de Haas oscillations in an $Al_{0.4}Ga_{0.6}N$/GaN heterostructure.** *J Appl Phys* 2003, **93:**2055.
47. Juang JR, Huang T-Y, Chen T-M, Lin M-G, Lee Y, Liang C-T, Hang DR, Chen YF, Chyi J-I: **Transport in a gated $Al_{0.18}Ga_{0.82}N$/GaN electron system.** *J Appl Phys* 2003, **94:**3181.
48. Chen JH, Lin JY, Tsai JK, Park H, Kim G-H, Youn D, Cho HI, Lee EJ, Lee JH, Liang C-T, Chen YF: **Experimental evidence for Drude-Boltzmann-like transport in a two-dimensional electron gas in an AlGaN/GaN heterostructure.** *J Korean Phys Soc* 2006, **48:**1539.
49. Cho KS, Huang T-Y, Huang CP, Chiu YH, Liang C-T, Chen YF, Lo I: **Exchange-enhanced g-factors in an $Al_{0.25}Ga_{0.75}N$/GaN two-dimensional electron system.** *J Appl Phys* 2004, **96:**7370.
50. Cho KS, Liang C-T, Chen YF, Tang YQ, Shen B: **Spin-dependent photocurrent induced by Rashba-type spin splitting in $Al_{0.25}Ga_{0.75}N$/GaN heterostructures.** *Phys Rev B* 2007, **75:**085327.
51. Lin S-K, Wu KT, Huang CP, Liang C-T, Chang YH, Chen YF, Chang PH, Chen NC, Chang C-A, Peng HC, Shih CF, Liu KS, Lin TY: **Electron transport in In-rich $In_xGa_{1-x}N$ films.** *J Appl Phys* 2005, **97:**046101.

doi:10.1186/1556-276X-8-307
Cite this article as: Lo *et al.*: Tunable insulator-quantum Hall transition in a weakly interacting two-dimensional electron system. *Nanoscale Research Letters* 2013 **8**:307.